N- and C-Terminal Hydrophobic Patches Are Involved in Fibrillation of Glucagon†

Jesper Søndergaard Pedersen,‡ Dancho Dikov,§ and Daniel Erik Otzen*,‡

Center for Insoluble Protein Structures (inSPIN), Department of Life Sciences, Aalborg University, Sohngaardsholmsvej 49, DK-9000 Aalborg, Denmark, and Novo Nordisk A/S, Brogaardsvej 66, DK-2820 Gentofte, Denmark

Received June 20, 2006; Revised Manuscript Received September 30, 2006

ABSTRACT: Recent work suggests that the molecular structure of amyloid-like fibrils is determined by environmental conditions as well as amino acid sequence. To probe the involvement of side chains in fibrillation of the 29-residue hormone glucagon, we have measured fibrillation kinetics of 15 alanine mutants. At acidic pH, all of the mutants are able to form fibrils. However, substitution of hydrophobic residues in the N- and C-termini (in particular Phe6, Tyr10, Val23, and Met27) decelerates fibrillation dramatically. This indicates that the hydrophobicity and/or high β-sheet propensity of these residues may be important for fibrillation. In contrast, substitution of Leu14 increases fibrillation propensity compared to that of the wild type. Nevertheless, despite identical fibrillation conditions, the thioflavin T and tryptophan fluorescence spectra of fibrils formed by mutants Tyr13, Leu14, and Asp15 are significantly different from those of other mutants, indicating that substitution of these residues may influence not only the fibrillation kinetics and fibril stability but also the preferred final structure of the fibrils that is formed, in line with the general structural polymorphism of glucagon fibrils. In contrast, under alkaline conditions, only a handful of the alanine mutants are capable of forming fibrils, suggesting that more side chains are involved in stabilizing interactions here. In addition, fibrils formed by wild-type glucagon at alkaline pH appear very stable, compared to fibrils formed at acidic pH. This suggests that the distribution of charges determines the number of different fibrillated states available to a peptide, since these can block formation of metastable fibrillated states.

A number of debilitating diseases appear to involve formation of cytotoxic aggregates of proteins that otherwise serve a benign function in the human body (*1*). Formation of highly ordered repetitive cross-β-sheet fibrillar structures, known as amyloid, is a hallmark of a subset of these diseases (*2*). In principle, the ability to form amyloid-like structures may be a generic property of the peptide chain itself (*3*); however, it is clear that some amino acid sequences have a higher propensity for fibril formation than others (*4*). Tragic genetic disorders may result from single-amino acid substitutions, which can severely increase symptoms as well as accelerate the onset of protein deposition diseases (*5*, *6*). Mutagenesis can be used to investigate which parts of a protein are involved in aggregation (*7*, *8*). Strategies involving systematic substitutions of, for example, alanine (*9*) or proline (*10*−*12*) can be used to probe the involvement of side chains or the backbone in fibrillar structures, respectively. Alternatively, if an efficient selection or screening assay is available, the sequence space can be investigated through random mutagenesis (*13*, *14*). Recently, results from a number of mutagenesis studies have been combined in an attempt to establish a unifying theory that allows prediction of the intrinsic fibrillation tendency of any given amino acid sequence (*15*−*18*). In conjunction with structural investigations, these studies have revealed that aromatic (*19*) and β-branched residues are important for β-aggregation and fibrillation (*16*). These approaches only attempt to predict the overall aggregation propensity or the fibril elongation rate; the lag time is assumed to be sensitive to sample handling conditions such as agitation which is difficult to parametrize.

In this study, we have investigated the fibrillation of 15 different alanine mutants of the 29-residue peptide hormone glucagon. Glucagon has been known to readily form fibrils under acidic and alkaline conditions for almost half a century (*20*−*23*). The structure of fibrils that is formed is highly dependent on extrinsic factors such as glucagon concentration, temperature, and ionic strength (*24*), but also on the nature of solvent ions (*25*). Several mutagenesis studies have focused on the biological activity of glucagon, which has revealed that N- and C-terminal helices are important for the binding of glucagon to its seven-transmembrane G-protein-coupled receptor (for a review, see ref *26*).

Our results from this fibrillation study of 15 alanine mutants suggests that two hydrophobic regions in the N- and C-termini are important for fibrillation under acidic conditions, since alanine substitutions in these regions lead to significantly increased lag times and lowered fibril stability. In contrast, the middle region (residues 13−18) and residue Phe22 seem more to influence the type of fibrils that are

† J.S.P. was supported by a Ph.D. stipend cofinanced by Aalborg University and Novo Nordisk A/S. D.E.O. is supported by the Danish Research Foundation (inSPIN) and the Villum Kann Rasmussen Foundation (BioNET).

* To whom correspondence should be addressed: Center for Insoluble Protein Structures (inSPIN), Department of Life Sciences, Aalborg University, Sohngaardsholmsvej 49, DK-9000 Aalborg, Denmark. Phone: +45 96 35 85 25. Fax: +45 98 14 18 08. E-mail: dao@bio.aau.dk.

‡ Aalborg University.

§ Novo Nordisk A/S.

10.1021/bi061228n CCC: $33.50
Published on Web 11/09/2006

formed. At alkaline pH, only five of the 15 mutants were able to grow into fibrils within 96 h, indicating that a larger number of side chain interactions are essential to fibril formation under alkaline conditions. This is consistent with the high stability of fibrils formed at this pH, which indicates that these fibrils are bound together through a multitude of stabilizing side chain interactions.

MATERIALS AND METHODS

Chemically synthesized glucagon mutants (said to be >95% pure by HPLC according to the manufacturer) were obtained from Biosyntan GmbH. Pharmaceutical-grade wild-type glucagon (>98.9% pure) was obtained from Novo Nordisk A/S (Bagsværd, Denmark). Thioflavin T (ThT) obtained from Sigma-Aldrich (St. Louis, MO) was used without further purification. Ultrapure guanidine hydrochloride (GdmCl) was obtained from Invitrogen (Carlsbad, CA). Glycine, HCl, and NaCl were obtained from AppliChem GmbH (Darmstadt, Germany).

Further Purification of Mutants with RP-HPLC. Our initial fibrillation kinetics trials revealed that the impurities left in the synthetic peptides decreased fibrillation rates dramatically compared to that of pharmaceutical-grade glucagon (Figure S1 of the Supporting Information). It has previously been reported that the speed of fibrillation of glucagon at acidic pH is dependent on the purity of the glucagon peptide (*20*). We therefore purified the mutants further using reverse phase HPLC (HP1100 Series, Agilent Technologies, Palo Alto, CA) on a Hibar LiChrosorp RP-18 (7 μm) 250 mm × 10 mm column. A single set of eluents [A being 20% acetonitrile and 0.1 M KH_2PO_4 (pH 2.7) and B being 40% acetonitrile] were used for all mutants. Generally, we used very shallow gradients where the end acetonitrile concentration was only ~2% higher than the starting concentration (e.g., gradient from 30 to 32% acetonitrile for wild-type glucagon). Analysis of the elution profiles revealed that most of the peptides were only >80% pure prior to purification.

Purified peptides were desalted by batch adsorption to Poros 50 R2 beads (PerSeptive Biosystems, Framingham, MA) and precipitation by centrifugation. The beads were washed three times with 10 mL of distilled water (maximum 250 μL residual volume between washes). Subsequently, the peptides were eluted with 2 × 1.3 mL of 50% acetonitrile and lyophilized overnight. To ensure a fair comparison, all peptides were subjected to the same purification and desalting steps. At the end of this step, the mutants were estimated to be ~97% pure.

Fibrillation Kinetics of Glucagon Mutants. To remove potential fibril seeds, the purified peptides were dissolved at a concentration of ~3 mM in 7 M GdmCl, which is expected to keep proteins and peptides in a monomeric random coiled state (*27*). The 7 M GdmCl stocks were flash-frozen in liquid nitrogen and stored at −80 °C when not in use. The mutant stocks were diluted to 50 μM in buffer and transferred to black polystyrene 384-well microtiter plates (Nunc GmbH & Co. KG, Wiesbaden, Germany). The plates were covered with crystal-clear sealing tape (Hampton Research, Aliso Viejo, CA) and placed in a Spectramax Gemini XS fluorescence plate reader. The plate reader was programmed to read fluorescence at 330 and 355 nm ($\lambda_{excitation}$ = 295 nm) and at 502 nm ($\lambda_{excitation}$ = 442 nm) at fixed intervals preceded by 60 s of automixing before every read. Noise-reduced fluorescence readings [generally the relation $F = Em_{355} - 0.48 \times Em_{330}$ was used at acidic pH and the relation $F = Em_{355} - 0.75 \times Em_{330}$ at pH 9.5, where Em_{355} and Em_{330} are the fluorescence intensities observed at 355 and 330 nm, respectively (*24*)] from every well were fitted to the following equation using our custom JSPK software (*24*):

$$F = (a_m + b_m t) + \frac{a_f + b_f t}{(1 + \upsilon e^{-k(t-t_m)})^{1/\upsilon}} \quad (1)$$

where F is the noise-reduced signal, a_x and $b_x t$ are linear equations describing the lag phase (m) and the equilibrium (f) baselines, t_m is the time point of maximum elongation rate, and υ describes the asymmetry of the sigmoidal curve. The elongation rate is given by $k/(1 + \upsilon)$, and the lag time is defined as $t_m - (1 + \upsilon)/k$, which is the time where the tangent at t_m crosses the lag phase baseline. The apparent fibrillation rate is defined as (lag time)$^{-1}$. For some mutants, one of four wells failed to give signs of fibrillation during the assay, while the remaining three exhibited similar fibrillation kinetics. For these mutants, the nonfibrillating wells were scored as statistical outliers and removed from the set.

All compared fibrillation kinetics in this article were obtained in single, parallel plate assays: one assay with 160 mM GdmCl at pH 2.5, one assay with 500 mM GdmCl at pH 2.5, and one assay with 160 mM GdmCl at pH 9.5.

Emission Wavelength Scan Analysis. Emission wavelength scans were recorded using the SpectraMAX plate reader with 5 nm increments. Data from the plate reader were imported into JSPK (*24*), and 50 nm windows around the maximum wavelengths were fitted to a third-order polynomial. The wavelength of maximum intensity (λ_{max}) was obtained by differentiating the obtained polynomial and solving the resulting second-order equation. λ_{max} values could generally be reproduced within ±1.5 nm (see Figure S3 of the Supporting Information).

Fibril Urea Dissociation Kinetics. Fibrils formed by glucagon mutants in the plate reader assay were diluted 2-fold in 10 M urea, and the resulting dissociation kinetics in 5 M urea were recorded by measuring emission at 330 and 355 nm every 30 s ($\lambda_{excitation}$ = 295 nm). To reduce signal noise, the emission at 355 nm was normalized with the emission at 330 nm, which remained relatively constant during the dissociation (data not shown). The resulting normalized fluorescence signal was fitted to a single exponential with a linear slope. The missing amplitude was calculated as the difference between the Em_{330}/Em_{355} ratio from the fluorescence wavelength scan taken immediately prior to addition of urea and the first time point in the kinetic run.

Fibrils formed by 1.3 mg/mL wild-type glucagon in 50 mM glycine/NaOH (pH 9.5) were diluted to variable urea concentrations in a 96-well black polystyrene plate (Costar, Corning Inc.). The final concentration of glucagon was 0.22 mg/mL. The plate was covered by with crystal-clear sealing tape and read every 133 s with 3 s of automixing prior to each read. The dissociation rate constants were calculated by fitting the normalized fluorescence signal (Em_{355}/Em_{330}) to a double-exponential equation. Urea dissociation midpoints

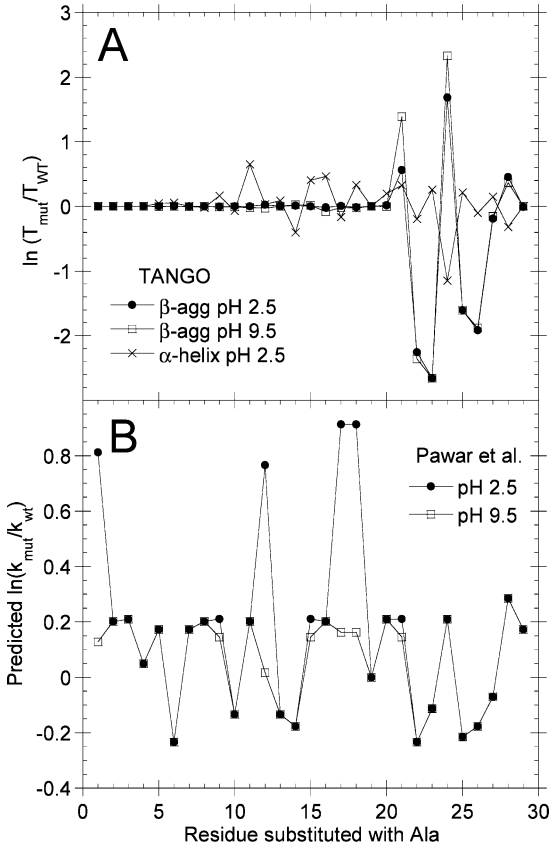

FIGURE 1: (A) Predicted β-aggregation (● and □) and α-helix (×) TANGO (*15*) score (T_{mut}) for alanine substitution mutants of glucagon compared to the wild type (T_{WT}) at pH 2.5 (● and ×) and pH 9.5 (□). All calculations were made with the ionic strength set to 0.15 M. Lines are provided for visual guidance only. (B) Predicted effects of alanine substitution on elongation rates calculated according to the method of Pawar et al. (*16*).

([urea]$_{50\%}$) were calculated from end point fluorescence and amplitudes by fitting to the following equation (*28*):

$$Y_{obs} = \frac{\alpha_N + \beta_N[\text{urea}] + (\alpha_U + \beta_U[\text{urea}]) \times 10^{m}\text{D}\cdot\text{N}^{([\text{urea}]-[\text{urea}]_{50\%})}}{1 + 10^{m([\text{urea}]-[\text{urea}]_{50\%})}} \quad (2)$$

RESULTS

Solid-State Synthesis Derivatives Impede Fibrillation of Glucagon. Because glucagon consists of only 29 residues, we used solid-state synthesis rather than using traditional cloning, mutagenesis, expression, and purification to generate glucagon mutants. A total of 15 alanine substitution mutants were synthesized, guided by predictions from the TANGO algorithm (*15*) (see Figure 1A), which prompted us to investigate the hydrophobic region spanning residues 22−27. We did not mutate Trp25, which is a convenient spectroscopic probe for detection of fibril formation (*24*). As controls, a number of residues outside the predicted fibrillogenic region were also mutated, using types of amino acids similar to those mutated in the region of residues 22−27. In addition, alanine mutants of Arg17 and Arg18, said to increase fibrillation tendency according to Pawar et al. (*16*), but not according to TANGO (see Figure 1), were included in the mutagenesis.

To benchmark the chemical synthesis, we compared the fibrillation kinetics of wild-type (WT) pharmaceutical-grade glucagon (>98.9% pure, produced by fermentation and purified by Novo Nordisk) to that of solid-state synthesized wild-type glucagon (WT*) (>95% pure by HPLC according to the manufacturers). To our surprise, WT* forms fibrils much slower than WT (Figure S1), despite the fact that both peptides had been incubated in 7 M GdmCl prior to fibrillation to dissolve potential fibril seeds in either stock. In addition to the lower purity, WT* also contains traces of trifluoroacetic acid from the HPLC purification. However, no trifluoroacetic acid salt concentrations between 0.1 and 250 mM could modulate the kinetics of the WT fibrillation to even remotely resemble that of WT* (Figure S1), suggesting that the impurities present in WT* were the reason for the slowed fibrillation. Indeed, a report from 1955 observes that the rate of fibrillation at acidic pH is highly dependent on the purity of glucagon (*20*). We therefore further purified all mutants using RP-HPLC (see Materials and Methods). To evaluate the effect of the purification step, fibrillation kinetics were measured before and after the purification. For six of seven tested mutants, the fibrillation kinetics of the purified peptides was much faster than that of the crude peptides (see Figure S2 of the Supporting Information).

Large Hydrophobic Residues Are Important for Fibril Formation of Glucagon. The alanine mutants were allowed to form fibrils at pH 2.5 and a peptide concentration of 50 μM. Because all peptides were dissolved in 7 M GdmCl to remove potential fibril seeds formed during purification, the dilution of the purified peptides resulted in two different concentrations (160 and 500 mM) of residual GdmCl. Previous results indicate that at 100 mM GdmCl, WT glucagon generally forms the low-thioflavin T (ThT) stainable type D fibrils (*24*), whereas the fibrils formed at the higher GdmCl concentrations generally stain better with ThT (*25*). In addition to ThT fluorescence (see the examples in Figure 2A), the emission intensity of Trp25 (see Figure 2B) was collected during a 96 h incubation at room temperature. As previously observed for WT glucagon (*24*), increases in ThT fluorescence, which are indicative of fibril formation, invariably occurred concurrently with distinct Trp emission blue shifts for all mutants. The fibrillation kinetics, deduced from the Trp traces, and ThT fluorescence onset times for all mutants are summarized in Table 1 and Figure 2C.

All alanine substitution mutants were able to form fibrils according to the increase in ThT fluorescence (see, e.g., Figure 2A). However, mutants YA10, VA23, MA27, and especially FA6 formed fibrils only after very long lag times (see Table 1). The FA6 mutant had the longest lag time, indicating that Phe6 is particularly important for the fibrillation. In contrast, substitution of the other Phe residue at position 22 had an only limited impact on the fibrillation rate despite the TANGO score which predicts a substantial reduction in the level of β-aggregate formation for FA22, although we should emphasize that TANGO does not make predictions about the actual lag times of fibrillation (Figure 1A). In general, substitution of the large hydrophobic residues prolonged the lag phase most, the clear exception being the LA14 mutant, which formed fibrils faster than WT glucagon. In addition, the other Leu mutant, LA26, was only slightly

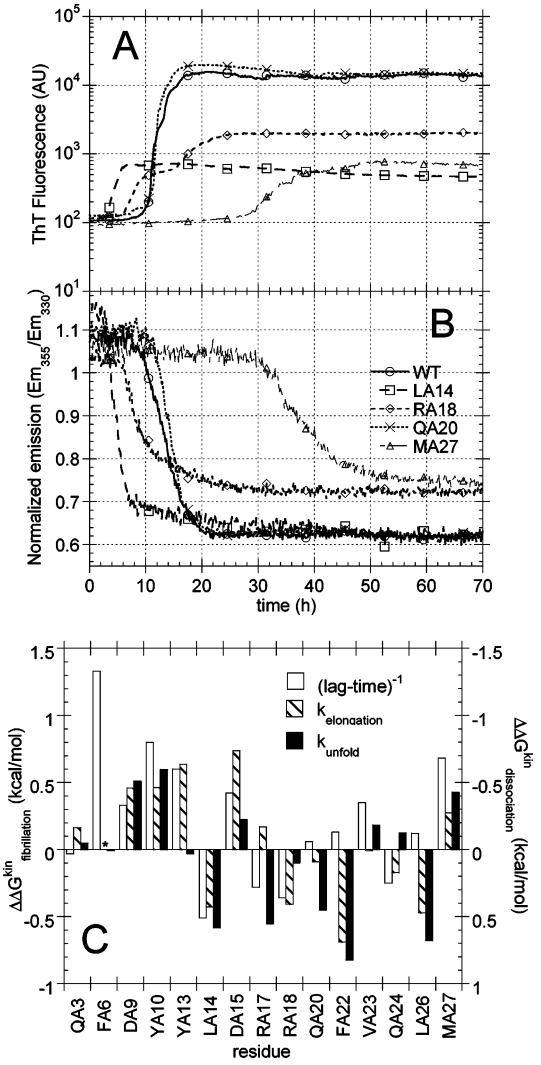

FIGURE 2: Fibrillation of 50 μM glucagon mutants in 50 mM glycine/HCl (pH 2.5) with 0.16 M GdmCL. (A) Representative ThT fluorescence time courses for WT glucagon (○) and mutants LA14 (□), RA18 (◇), QA20 (×), and MA27 (△). (B) Normalized Trp fluorescence (emission at 355 nm divided by the emission at 330 nm) observed for the same samples and the same times as in panel A. (C) Summary of observed fibrillation kinetics at 160 mM GdmCl given in terms of $\Delta\Delta G^{kin} = RT \ln(k_f^{WT}/k_f^{mut})$: elongation rates (hatched bars) and fibrillation rates [(lag time)$^{-1}$] (white bars) and fibril dissociation kinetics (black bars). See Figure 4 and the text for details on dissociation kinetics. Because the full transition was not observed for mutant FA6, the apparent elongation rate could not be estimated. Note that the right *y*-axis indicating the $\Delta\Delta G$ for fibril dissociation has been reversed to facilitate comparison with fibrillation kinetics, which occur in the reverse (aggregative) direction.

slower than WT, indicating that the two Leu residues are not critical to fibrillation.

Fluorescence Spectrum and ThT Staining Vary with the Position of the Substitution. Under acidic conditions, glucagon is known to form several different types of fibrillar aggregates (*24*), which exhibit highly variable ThT stainability depending on fibrillation temperature, peptide concentration, and salt concentration (*25*). After fibrillation for 96 h, fluorescence emission spectra were recorded for all mutants (examples of these are shown in Figure 3A). In contrast to the uniform fluorescence spectrum of the monomeric peptides (recorded before incubation), which all had emission maxima (λ_{max}) at ~350 nm (Figure 3B), the fluorescence spectrum of the fibrillated mutants was much more variable, especially for the mutants fibrillated at high GdmCl concentrations. Although all mutants generally exhibited blue shifting of Trp emission, the end point fluorescence intensities and λ_{max} varied considerably. For mutants 13−15, the fluorescence intensity was doubled upon fibrillation and λ_{max} was only blue-shifted to 332 nm (Figure 3C). The increased Trp fluorescence intensity compared to that of WT glucagon is at least partly due to the absence of Föster resonance energy transfer (FRET) (*29*) from the Trp to the ThT for the fibrillated states of these peptides (*25*). This is seen from the general trend that mutants with a high ThT content also have a low Trp content (compare panels C and D of Figure 3) and vice versa. A similar FRET from Trp to ThT has been observed for fibrils of human apolipoprotein C-II (*30*). In addition to variation in the λ_{max} of Trp emission, there was also a smaller variation in ThT emission (see Figure S3 of the Supporting Information). However, the spectra exhibited no correlation between the λ_{max} values for ThT and Trp emissions.

Alanine Substitutions Affect Fibril Stability. The mutants were allowed to grow into fibrils for an additional 2 months without agitation. The extra incubation changed the fluorescence spectrum considerably. All mutants now exhibited emission maxima around 318−330 nm (an average of 321.8 ± 3.3 nm), which is significantly shifted compared to the value of 332.1 ± 11.5 nm measured right after the 96 h incubation. The changed fluorescence spectrum is consistent with a slow fibrillation of mutants, which did not form fibrils during the 96 h incubation, in addition to a slow conversion of rapidly formed metastable fibrils into more stable and Trp-emission-blue-shifted fibrils [e.g., type B (*24*)] over time. To estimate the stability of fibrils that formed, we diluted fibrils 2-fold with 10 M urea, giving a final urea concentration of 5 M, and measured the change in Trp emission over time (Figure 4). The change in normalized Trp emission followed an exponential decay, consistent with a first-order dissolution and unfolding of aggregated material as seen previously (*24*).

The observed dissociation rates are summarized in Table 2 and Figure 2C. Interestingly, the slowest dissociation rate constants were observed for FA22. Together with the lower end point fluorescence, this indicates that fibrils formed by this mutant are much more stable than those formed by WT glucagon and the other mutants. It has previously been shown that the stability of glucagon fibrils is highly dependent on how challenging the conditions were when they were formed (*24*). For example, fibrils formed at high temperatures are more stable than those formed at low temperatures. This means that the high stability of the FA22 fibrils may be a result of challenging fibrillation conditions which could arise if truncation of the Phe22 side chain prevents formation of metastable fibrils. Nevertheless, the high stability indicates that the Phe22 residue is not essential for the structural packing of glucagon fibrils. A similar slowed dissociation rate compared to that of WT is seen for the fibrils of mutants LA14, RA17, and LA26. In contrast, the slow fibrillating mutants FA6, YA10, VA23, and MA27 all have very fast dissociation rates or small amplitudes, indicating that the fibrils that do form are not very stable.

Only a Few Alanine Mutants Are Able To Form Fibrils at Alkaline pH. WT glucagon is able to form fibrils quite

Table 1: Summary of Fibrillation Kinetics for Alanine-Substituted Glucagon Mutants in 50 mM Glycine/HCl (pH 2.5)

	lag time (h)[a]		elongation rate (min^{-1})		ThT onset time (h)[b]	
	500 mM GdmCl	160 mM GdmCl	500 mM GdmCl	160 mM GdmCl	500 mM GdmCl	160 mM GdmCl
WT	11.1 ± 4.2	10.5 ± 2.02	28.3 ± 6.4	22.0 ± 6.2	10.0 ± 4.3	11.9 ± 1.5
QA3	7.8 ± 2.7	10.0 ± 1.5	14.2 ± 7.2	16.6 ± 2.5	9.1 ± 1.1	9.4 ± 3.1
FA6	>70	>96	NA[c]	NA[c]	>70	>96
DA9	31.5 ± 1.7	18.3 ± 3.4	11.8 ± 1.3	10.1 ± 2.8	23.5 ± 6.7	20.8 ± 2.2
YA10	32.1 ± 2.6	40.6 ± 2.9	7.5 ± 0.6	10.0 ± 1.9	34.7 ± 2.3	42.9 ± 4.8
YA13	19.1 ± 6.8	29.1 ± 3.7	16.1 ± 1.2	7.5 ± 0.6	19.9 ± 6.1	32.8 ± 3.2
LA14	7.6 ± 5.7	4.4 ± 0.1	20.1 ± 8.6	45.0 ± 5.1	8.1 ± 4.4	4.5 ± 1.6
DA15	7.2 ± 5.1	21.3 ± 2.8	13.0 ± 2.8	6.3 ± 3.6	11.9 ± 8.8	20.3 ± 1.2
RA17	5.1 ± 0.4	6.6 ± 2.0	16.8 ± 3.0	16.5 ± 6.6	6.9 ± 0.7	7.1 ± 2.5
RA18	7.2 ± 1.2	5.7 ± 1.0	25.4 ± 7.7	43.7 ± 8.8	10.1 ± 1.6	8.1 ± 1.1
QA20	14.4 ± 1.2	11.7 ± 0.8	26.6 ± 12.4	25.6 ± 3.2	14.4 ± 0.5	10.8 ± 0.8
FA22	19.1 ± 1.0	13.1 ± 1.0	28.4 ± 10.7	70 ± 11	18.4 ± 2.3	13.9 ± 0.1
VA23	34.8 ± 2.6	18.9 ± 1.1	NA[c]	22.3 ± 9.0	36.9 ± 4.3	28.7 ± 2.8
QA24	8.9 ± 0.8	6.8 ± 0.8	17.0 ± 3.4	29.4 ± 6.0	9.0 ± 1.5	10.3 ± 0.9
LA26	16.8 ± 3.3	12.9 ± 2.0	9.3 ± 3.2	49 ± 11	24.7 ± 3.4	14.4 ± 2.4
MA27	42.0 ± 9.9	33.2 ± 4.1	NA[c]	13.8 ± 6.8	37.6 ± 11.0	36.0 ± 7.8

[a] Lag times and apparent elongation rates were calculated by fitting Trp emission to eq 1. The error stated is the standard deviation of three or four replicate wells. [b] ThT onset time is the time at which the intensity reaches 250 RFU. [c] Complete transition not observed.

readily at pH 9.5 (*25*). In contrast, only a few of the alanine substitution mutants were able to form fibrils during a 96 h incubation at pH 9.5 (see Table 3). This indicates that many of the substituted residues are important for the packing of the fibril structure at alkaline pH. As seen at acidic pH, Ala substitutions at positions 14 and 26 do not prevent fibrillation, indicating that these two hydrophobic Leu residues are not critical for fibrillation. Interestingly, mutation of the two Arg residues appears to prevent fibrillation of glucagon. One could speculate that the Arg side chains may be involved in salt bridging in fibrillated glucagon at pH 9.5.

Wild-Type Glucagon Fibrils Formed at pH 9.5 Are Much More Stable than Those Formed in Acid. It has previously been shown that the stability of glucagon fibrils can be estimated using both thermal scanning CD and chemical denaturation (*24*). While sonicated fibrils formed at low pH are highly soluble, possibly because of the approximately +5 charge per molecule, the fibrils formed at pH 9.5 (approximately −1 charge per molecule) have a very poor solubility, which is an obstacle to CD-based thermal scans. We have therefore estimated the stability of WT glucagon fibrils formed at pH 9.5 by chemical denaturation using urea. Because of the very slow dissociation of fibrils in urea, we monitored the change in Trp emission over time to ensure that the reaction reached equilibrium. The dissociation of the fibrils proceeded in a manner described well by a double-exponential decay of the fibrils (Figure 5A). Both the exponential amplitudes and end point fluorescence levels reveal a clear cooperative transition from a fibrillar state to the monomeric state as the urea concentration increases (Figure 5B). All these transitions have similar dissociation midpoints, $[urea]_{50\%}$ of 5.5−5.7 M urea, and similar m values ($m_{amp1} = 0.35 \pm 0.01$; $m_{amp2} = 0.44 \pm 0.06$; $m_{end-point} = 0.36 \pm 0.01$), indicating that they originate from the same transition (Figure 5C). The dissociation midpoints are significantly larger than the $[urea]_{50\%}$ values of 3.5 M ($m_{end-point} = 0.59$) observed for even the most stable, type C, fibrils observed at pH 2.5 and high temperatures (*24*). In fact, type B fibrils formed at ambient temperature at pH 2.5 have a $[urea]_{50\%}$ value of only 2.2 M ($m_{end-point} = 0.89$) (*24*). As seen in Figure 5B, the faster of the two observed dissociation rate constants decreases with urea concentration up to around 6 M urea, above which it starts to increase slightly. This is analogous to the situation for folding and unfolding of globular proteins as a function of denaturant concentration; below the denaturation midpoint, the observed rate constant (dominated by refolding) decreases with an increase in denaturant concentration, while the opposite is the case above the midpoint (dominated by unfolding). In the case of the glucagon fibrils, even though we are monitoring a dissociation process at all urea concentrations (akin to unfolding), the observed rate constant is the sum of the dissociative and associative rate constants; the associative rate constant must be faster, although it decreases with urea concentration.

DISCUSSION

Comparison with Predicted Values Emphasizes (Un)-important Regions of Glucagon. Pawar et al. have recently proposed that relative fibrillation rates can be calculated by a simple formula (*16*), based on a compilation of elongation rate constants of various protein mutants, obtained without agitation (*17*). By specifying a sequence length of one, this formula assigns an amyloid propensity score for each of the 20 naturally occurring amino acids. Of these, the aromatic side chains generally have the highest propensities, consistent with recent structural investigations of fibrils (*19*). With six aromatic residues, His1, Phe6, Tyr10, Tyr13, Phe22, and Trp25, in a sequence of just 29 amino acids (*31*), glucagon can be considered rich in such amyloid prone residues.

We have applied the Pawar algorithm (*16*) to predict the effects of alanine substitutions on glucagon at both pH 2.5 and 9.5. As shown in Figure 1A, the algorithm generally predicts that substitution of hydrophobic residues decelerates fibrillation, whereas substitution of other residues is predicted to accelerate fibrillation. Interestingly, the predicted elongation rate constants for the glucagon mutants used in this study show no correlation with the observed rate constants (Figure 6A; $R^2 < 0.072$). Many types of glucagon fibrils grow exponentially due to the existence of secondary pathways (*24*). This means that differences in the duration of the lag phase can result both from changes in the overall elongation rate (including secondary pathways) and from shifts in

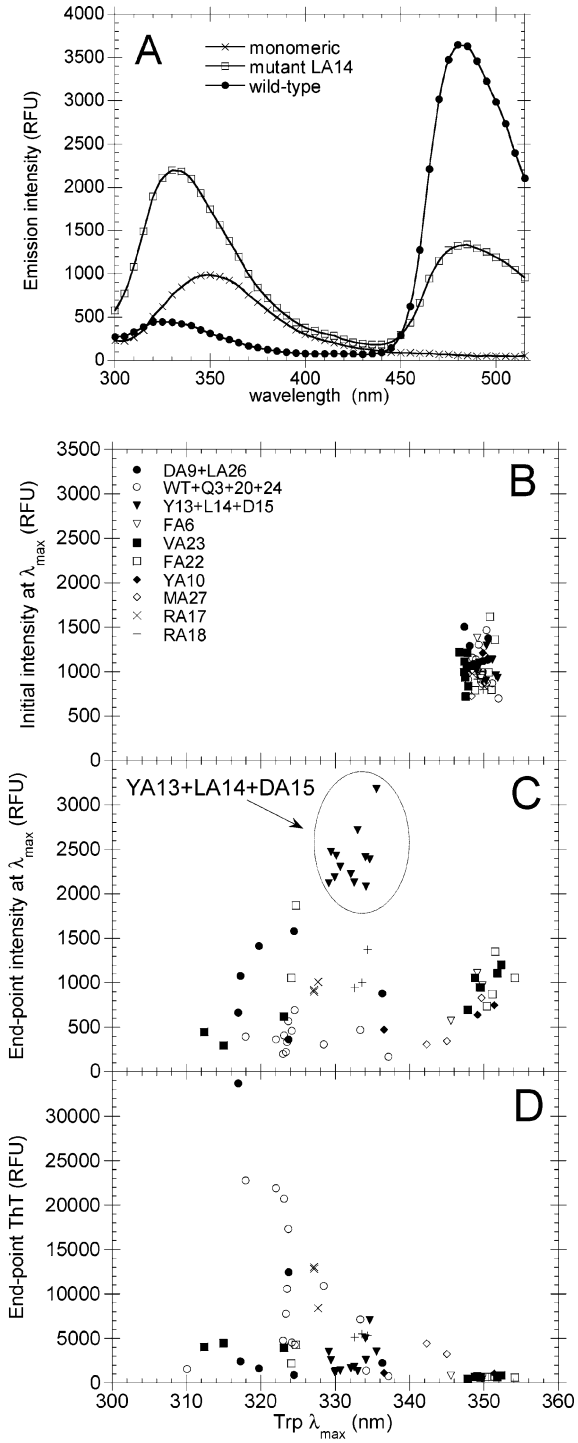

FIGURE 3: (A) Examples of representative fluorescence wavelength scans for fibrils formed by WT (●) and mutant LA14 (□) compared to that of the monomeric peptide (×) in 50 mM glycine/HCl (pH 2.5) with 500 mM GdmCl. (B) Analysis of the initial fluorescence spectrum for all samples given plotting the maximum Trp emission intensity as a function of wavelength of maximum intensity for mutants DA9 and LA26 (●), WT, QA3, QA20, and QA24 (○), YA13, LA14, and D15 (▼), FA6 (▽), VA23 (■), FA22 (□), YA10 (◆), MA27 (◇), RA17 (×), and RA18 (+). (C) Same as panel B but after incubation for 96 h. (D) Maximum ThT emission intensity of the same samples incubated for 96 h as a function of the wavelength of maximum Trp emission.

nucleation rates (*32*). In fact, there is often a simple linear correlation between the elongation rate and the fibrillation rate [calculated as (lag time)$^{-1}$] (*33*). When comparing the Pawar predicted rates to the observed fibrillation rates, we

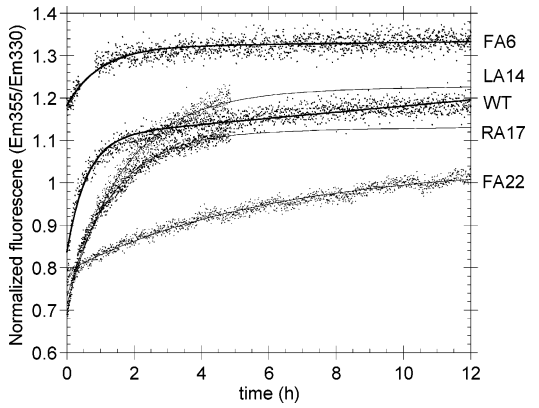

FIGURE 4: Examples of time-based dissociation profiles for fibrils in 5 M urea and 25 mM glycine (pH 2.7). Fibrils were formed by 50 μM peptide in 50 mM glycine/HCl (pH 2.5) with 0.16 M GdmCl.

Table 2: Observed Fibril Dissociation Rates upon Dilution to 5 M Urea in 25 mM Glycine/HCl (pH 2.7)

	k_{obs} (h^{-1})[a]	amplitude[a]	missing amplitude[b]	end point fluorescence[c]
WT	1.79	0.30	0.30	1.22
QA3	1.95	0.30	0.29	1.29
FA6	1.76	0.13	0.34	1.35
DA9	4.24	0.32	0.28	1.34
YA10	4.90	0.28	0.22	1.39
YA13	1.70	0.29	0.30	1.33
LA14	0.67	0.45	0.08	1.24
DA15	2.61	0.41	0.28	1.38
RA17	0.70	0.39	0.16	1.12
RA18	1.52	0.20	0.30	1.18
QA20	0.84	0.40	0.23	1.25
FA22	0.16	0.25	0.21	0.98
VA23	2.43	0.32	0.32	1.27
QA24	2.21	0.14	0.42	1.27
LA26	0.57	0.23	0.23	1.13
MA27	3.67	0.13	0.36	1.10

[a] k_{obs} and amplitude are calculated from a single-exponential fit to the observed transition. [b] Missing amplitude is the amplitude missing compared to a wavelength scan made just before the urea dilution. [c] Emission intensities after 12 h given as the intensity at 355 nm normalized to that at 330 nm.

also generally find a large deviation between the absolute values (Figure 6A). However, although the algorithm is not intended for predicting changes in (lag time)$^{-1}$, the correlation is better than with the elongation rates (see Figure 6B; $R^2 > 0.41$). Mutants LA14 and FA22 generally appear to grow into fibrils much faster than predicted; if these mutants are removed from the comparison, the correlation is slightly better ($R^2 > 0.61$ and 0.66 for 0.50 and 0.16 M GdmCl, respectively).

Compared to the predictions by TANGO (*15*) (see Figure 1), the Pawar algorithm appears to better predict the experimentally observed importance of residues FA6 and YA10, which are scored as relatively unimportant by TANGO. However, none of the two prediction algorithms are capable of predicting that substitution of Leu14 actually accelerates fibrillation.

The folding pathway of monomeric proteins can be investigated by studying the effects of side chain truncation on folding−unfolding kinetics via Φ value analysis (*34*). In theory, analogous calculations could provide valuable differentiation for which residues are involved in nucleation and fibril stability, even though fibrillation is fundamentally

Table 3: Fibrillation Kinetics for Mutants Fibrillated at pH 9.5[a]

	lag time (h)[b]	ThT onset (h)	k_{app} (min^{-1})[c]
WT	6.7 ± 1.3	8.5 ± 0.5	59.8 ± 24.8
QA3		85.0 ± 7.9	
FA6			
DA9	15.7 ± 1.1	15.4 ± 1.0	20.4 ± 1.9
YA10			
YA13			
LA14	19.9 ± 5.0	20.3 ± 4.6	12.7 ± 1.2
DA15			
RA17			
RA18			
QA20	7.1 ± 0.8	9.3 ± 0.9	22.2 ± 7.5
FA22			
VA23			
QA24	49.7 ± 12.0	62.0 ± 18.7	14.4 ± 3.3
LA26	17.7 ± 4.3	17.1 ± 3.6	18.0 ± 1.4
MA27			

[a] Assay conditions: 50 μM mutant, 50 mM glycine/NaOH, pH 9.5, 160 mM GdmCl. [b] Lag times and apparent elongation rates were calculated by fitting the Trp emission to eq 1. The error stated is the standard deviation of three or four replicate wells. [c] ThT onset time is the time at which the intensity reaches 250 RFU.

different from folding of monomeric proteins. However, when we attempted such calculations from the kinetic data obtained in this study, the Φ values exhibited a high degree of scattering (data not shown), which prevented us from drawing a clear picture of the contributions of different residues to the fibrillation reaction. Since glucagon is capable of forming several different types of fibrils (*24*), it is possible that this scattering results from the alanine substitutions affecting relative populations of the various types of fibrils.

Effects of pH on Fibril Structure. At acidic pH, most if not all mutants were capable of forming some sort of Trp-emission-blue-shifted aggregates. The fact that all of the aggregates also exhibited some, albeit variable, ThT staining suggests that they are of an amyloid-like nature. In contrast, only a handful of the alanine mutants that were tested were capable of forming ThT stainable/Trp-blue-shifted aggregates at alkaline pH. Furthermore, the concentration of urea required to achieve 50% dissociation of the fibrils formed at pH 9.5 (~5.6 M urea) is significantly higher than the value of ~3.5 M required for even the most stable type of fibrils characterized so far at acidic pH (*24*). Taken together, these observations indicate that fibrils formed at pH 9.5 are formed in a very cooperative fashion and are stabilized by a larger number of favorable side chain interactions than their pH 2.5 counterparts. So far, we have observed four or five different types of WT glucagon fibrils that are each characterized by differences in ThT staining, CD/ATR-FTIR spectrum, and resistance to thermal melting (*24*, *25*). In theory, it is possible that even more stable fibril packing motifs could exist at acidic pH, the formation of which is repressed by less stable but kinetically more accessible fibrillated states. Apart from the differences in H^+, OH^-, and counterion concentrations, the pH change from 2.5 to 9.5 also modulates the charge distribution on the glucagon peptide (Figure 7). The major difference between the two pH values is the protonation state of the three Asp residues. When the pH is decreased, all three side chains are protonated, replacing three negative charges with three polar side chains capable of hydrogen bonding. Thus, it is tempting to speculate that the negative charges of the three Asp residues at pH 9.5 could function as "gatekeeper" residues

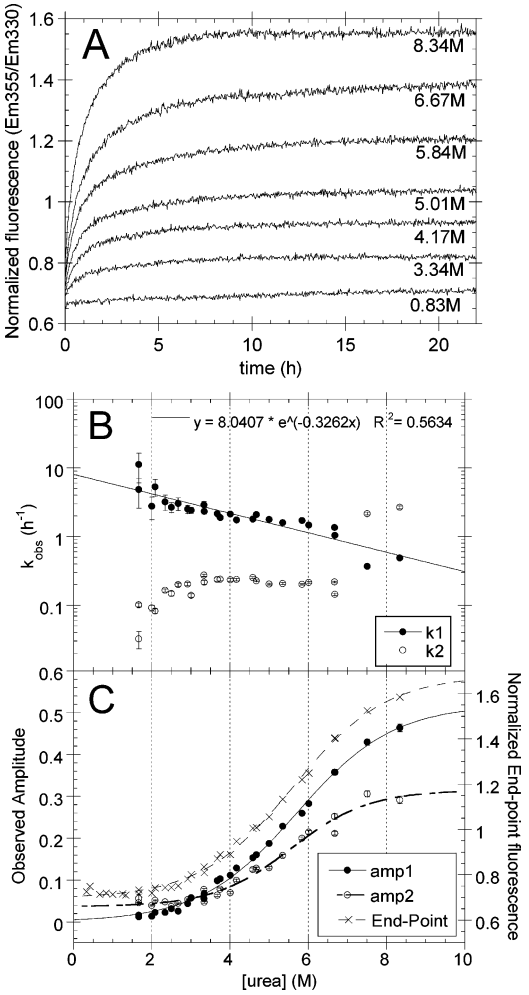

FIGURE 5: (A) Examples of time-based fluorescence traces during the dissociation of 0.22 g/L WT fibrils in 50 mM glycine/NaOH (pH 9.5) in variable concentrations of urea. Fibrils were formed by incubating 1.3 g/L glucagon for 24 h in 50 mM glycine/NaOH (pH 9.5) with shaking at 990 rpm. (B) Fast [k_1 (●)] and slow [k_2 (○)] observed dissociation rate constants from a least-squares double-exponential fit to the observed traces. (C) Amplitudes of fast (●) and slow (○) phases, from fitting to double-exponential and end point normalized fluorescence (×). Lines indicate fitting to the two-state dissociation model given in eq 2.

(*35*) that block formation of some of the metastable fibril types seen at pH 2.5. However, neither of the two Asp mutants tested in this study exhibited increased fibrillation propensities at pH 9.5. In fact, DA15 did not form fibrils at all, while DA9 fibrillated 2−3-fold more slowly than the wild type (Table 3). The pH change does not affect the positive charge on Lys12 and Arg17/18. However, while the alanine substitution at position 17 or 18 does not significantly alter the fibrillation kinetics at pH 2.5, these two mutants failed to form fibrils at pH 9.5. This contradicts the predictions of Pawar et al. (see Figure 6A) and suggests that the charges on residues 17 and 18 may be involved in vital salt bridges with the Asp residues or the C-terminus in the pH 9.5 fibrils.

At Acidic pH, Key Residues Fall into Two Contiguous Regions. It has recently been reported that secretin, a member of the glucagon superfamily with a sequence 52% identical to that of glucagon (*36*), does not form fibrils (*37*). Compared to glucagon, secretin has a number of aromatic residues substituted. Tyr10, Tyr13, and Phe22 are replaced with Leu,

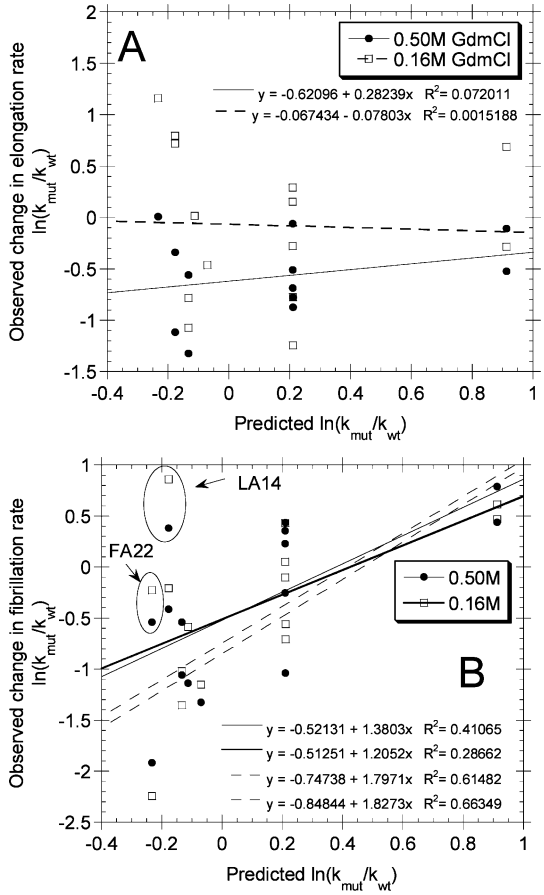

FIGURE 6: Comparison of the observed fibrillation kinetics with the predicted effects of alanine substitution on elongation rates calculated according to the method of Pawar et al. (*16*) for 0.50 M GdmCl (●) and 0.16 M GdmCl (□). (A) Comparison with the observed elongation rates (i.e., the highest observed slope). Lines represent the best linear fits. (B) Comparison with the observed fibrillation rates calculated as $(\text{lag time})^{-1}$. Solid lines indicate best linear fits of all points; dashed lines indicate best linear fits without considering highlighted points.

```
          ppp phpppphpphhpppphpphhphhhpp   Net charge
pH 2.5 : ++          +    ++               5+
         *HSQGTFTSDYSKYLDSRRAQDFVQWLMNT*
pH 9.5 :          -~ +~ - ++  -        -  1-
```

FIGURE 7: Theoretical distribution of charges on the glucagon peptide at pH 2.5 and 9.5. p stands for polar and h for hydrophobic.

and Trp25 is replaced with Gly. Judging from the dramatic blue shifting of the fluorescence spectrum [λ_{max} shifts from 352 to 318 nm (*24*)], Trp25 of glucagon becomes buried in a hydrophobic core upon fibrillation. Together with the fact that Trp residues have been assigned the highest theoretical propensity for amyloid formation (*16*), this implies that Trp25 could be very important for fibrillation of glucagon. Because we have relied on the fluorescence of its indole ring for following fibrillation, Trp25 was the only hydrophobic residue omitted from our alanine scanning, yet because of the alternating conformation of β-sheets, the side chain of Trp25 is expected to occupy the space between the important side chains of residues Val23 and Met27 in the fibrillated state, provided that this region is in fact in a β-strand configuration in the fibrillated state(s) of glucagon. In contrast, residues Phe22, Gln24, and Leu26, which are expected to be situated on the other side of the β-sheet, do not appear to be critical for fibril formation or stability. Early studies on monomeric glucagon have suggested that the

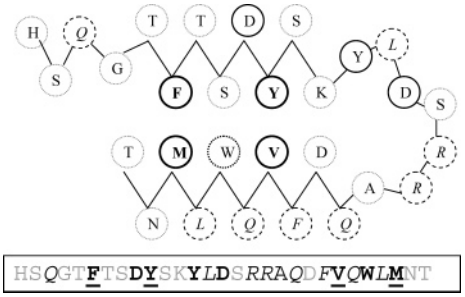

FIGURE 8: Summary of the effect of alanine substitutions on glucagon fibrillation at acidic pH: (gray dotted circles) not tested, (thin dashed lines) weak effects with a side chain of little importance, (thick lines with bold letters) important for fibrillation/fibril stability, (solid lines) important for some fibril types, and (thick dotted line) Trp25. Secondary structure and relative positions of residues implied in this model are not substantiated by the results of this study.

C-terminal part of the peptide is involved in a partial α-helical structure (*38*). Since both VA23 and MA27 substitutions are expected to increase α-helix propensity while the FA22, QA24, and LA26 decrease it [according to TANGO (*15*); see Figure 1A], it is possible that the stability of this helix may affect the fibrillation propensity of the whole peptide.

At the other end of the sequence, residues Phe6 and Tyr10 also appear to be very important for fibrillation of glucagon. If this region is in a β-strand configuration, these two residues will also be situated on the same side of the strand, separated by a single serine residue. Phe6 is flanked at positions 5 and 7 by Thr residues, which have high β-sheet propensities (*39*).

In the middle of the sequence, residues Tyr13 and Asp15 are more important under low-salt than under high-salt conditions. These two residues flank Leu14, truncation of which actually accelerates fibrillation in contrast to the predictions (see Figure 1). Furthermore, mutagenesis of residues 13−15 apparently affected the spectroscopic properties of the fibrils, producing fibrils with weak ThT staining and intense Trp emission. This suggests that these residues could play a key role in determining which type of fibril packing is preferred by the peptide. For example, one could speculate that the truncation of these residues may prevent formation of some types of fibrils or allow the glucagon mutants to form distinct fibrillar states.

Three decades ago, Chou and Fasman (*40*) applied their novel secondary structure prediction algorithm to the amino acid sequence of glucagon. The original algorithm predicts two β-sheet regions in the gel state of glucagon comprising residues 5−10 and 19−27. Furthermore, it predicts that substitution of residues Phe6 and Val23 with Glu would significantly reduce the stability of the β-sheet in glucagon (*40*). Our data suggest that there are two important fibrillation regions, namely around residues 6−10 and 23−27. In contrast, residues between these groups have minor effects on fibril stability and may therefore be relatively flexible. We are aware that glucagon is a peptide capable of forming a multitude of different amyloid-like structures (*24*). One possible structure of glucagon fibrils based on the data derived from this mutagenesis study could involve a loop joining the two important regions (Phe6 and Tyr10, and Val23, Trp25, and Met27) in a hydrophobic fibril core

(Figure 8). However, many other interaction modes are possible. Further alanine mutagenesis of the 12 remaining residues (not counting residue Ala19) could in principle shed more light on the structure of glucagon fibrils. However, in light of the potential differences between the preferred final structures of mutant versus wild-type glucagon fibrils, it will probably prove much more valuable to study the fibrillar structures of wild-type glucagon using solid-state NMR or X-ray diffraction methods.

ACKNOWLEDGMENT

Assistant Professor Guy Bauw is thanked for invaluable assistance on peptide HPLC purification and desalting. Amol Pawar is acknowledged for calculating the predicted fibrillation rate constants for glucagon.

SUPPORTING INFORMATION AVAILABLE

Effect of solid-state synthesis-derived impurities on glucagon fibrillation (Figure S1), effect of purification on glucagon mutants (Figure S2), and investigation of ThT emission spectra of glucagon mutants (Figure S3). This material is available free of charge via the Internet at http://pubs.acs.org.

REFERENCES

1. Selkoe, D. J. (2003) Folding proteins in fatal ways, *Nature 426*, 900−904.
2. Glenner, G. G., Eanes, E. D., Bladen, H. A., Linke, R. P., and Termine, J. D. (1974) β-Pleated sheet fibrils. A comparison of native amyloid with synthetic protein fibrils, *J. Histochem. Cytochem. 22*, 1141−1158.
3. Dobson, C. M. (1999) Protein misfolding, evolution and disease, *Trends Biochem. Sci. 24*, 329−332.
4. Lopez De La Paz, M., Goldie, K., Zurdo, J., Lacroix, E., Dobson, C. M., Hoenger, A., and Serrano, L. (2002) De novo designed peptide-based amyloid fibrils, *Proc. Natl. Acad. Sci. U.S.A. 99*, 16052−16057.
5. Goate, A., Chartier-Harlin, M. C., Mullan, M., Brown, J., Crawford, F., Fidani, L., Giuffra, L., Haynes, A., Irving, N., James, L., et al. (1991) Segregation of a missense mutation in the amyloid precursor protein gene with familial Alzheimer's disease, *Nature 349*, 704−706.
6. Chen, S., Ferrone, F. A., and Wetzel, R. (2002) Huntington's disease age-of-onset linked to polyglutamine aggregation nucleation, *Proc. Natl. Acad. Sci. U.S.A. 99*, 11884−11889.
7. Chiti, F., Taddei, N., Bucciantini, M., White, P., Ramponi, G., and Dobson, C. M. (2000) Mutational analysis of the propensity for amyloid formation by a globular protein, *EMBO J. 19*, 1441−1449.
8. Pedersen, J. S., Christensen, G., and Otzen, D. E. (2004) Modulation of S6 fibrillation by unfolding rates and gatekeeper residues, *J. Mol. Biol. 341*, 575−588.
9. Zanuy, D., Porat, Y., Gazit, E., and Nussinov, R. (2004) Peptide sequence and amyloid formation. Molecular Simulations and experimental study of a human islet amyloid polypeptide fragment and its analogs, *Structure 12*, 439−455.
10. Chiba, T., Hagihara, Y., Higurashi, T., Hasegawa, K., Naiki, H., and Goto, Y. (2003) Amyloid fibril formation in the context of full-length protein: Effects of proline mutations on the amyloid fibril formation of β2-microglobulin, *J. Biol. Chem. 278*, 47016−47024.
11. Wood, S. J., Wetzel, R., Martin, J. D., and Hurle, M. R. (1995) Prolines and amyloidogenicity in fragments of the Alzheimer's peptide β/A4, *Biochemistry 34*, 724−730.
12. Williams, A. D., Portelius, E., Kheterpal, I., Guo, J. T., Cook, K. D., Xu, Y., and Wetzel, R. (2004) Mapping Aβ amyloid fibril secondary structure using scanning proline mutagenesis, *J. Mol. Biol. 335*, 833−842.
13. Wurth, C., Guimard, N. K., and Hecht, M. H. (2002) Mutations that reduce aggregation of the Alzheimer's Aβ42 peptide: An unbiased search for the sequence determinants of Aβ amyloidogenesis, *J. Mol. Biol. 319*, 1279−1290.
14. Kim, W., and Hecht, M. H. (2005) Sequence determinants of enhanced amyloidogenicity of Alzheimer Aβ42 peptide relative to Aβ40, *J. Biol. Chem. 280*, 35069−35076.
15. Fernandez-Escamilla, A. M., Rousseau, F., Schymkowitz, J., and Serrano, L. (2004) Prediction of sequence-dependent and mutational effects on the aggregation of peptides and proteins, *Nat. Biotechnol. 22*, 1302−1306.
16. Pawar, A. P., Dubay, K. F., Zurdo, J., Chiti, F., Vendruscolo, M., and Dobson, C. M. (2005) Prediction of "Aggregation-prone" and "Aggregation-susceptible" Regions in Proteins Associated with Neurodegenerative Diseases, *J. Mol. Biol. 350*, 379−392.
17. DuBay, K. F., Pawar, A. P., Chiti, F., Zurdo, J., Dobson, C. M., and Vendruscolo, M. (2004) Prediction of the absolute aggregation rates of amyloidogenic polypeptide chains, *J. Mol. Biol. 341*, 1317−1326.
18. Chiti, F., Stefani, M., Taddei, N., Ramponi, G., and Dobson, C. M. (2003) Rationalization of the effects of mutations on peptide and protein aggregation rates, *Nature 424*, 805−808.
19. Makin, O. S., Atkins, E., Sikorski, P., Johansson, J., and Serpell, L. C. (2005) Molecular basis for amyloid fibril formation and stability, *Proc. Natl. Acad. Sci. U.S.A. 102*, 315−320.
20. Staub, A., Sinn, L., and Behrens, O. K. (1955) Purification and crystallization of glucagon, *J. Biol. Chem. 214*, 619−632.
21. Beaven, G. H., Gratzer, W. B., and Davies, H. G. (1969) Formation and structure of gels and fibrils from glucagon, *Eur. J. Biochem. 11*, 37−42.
22. Linke, R. P., Eanes, E. D., Termine, J. D., Bladen, H. A., and Glenner, G. G. (1976) Formation of amyloid-like fibrils from insulin and glucagon in vitro, in *Amyloidosis: Proceedings of the Fifth Juselius Foundation Symposium* (Wegelius, O., and Pasternack, A., Eds.) pp 371−373, Academic Press, London.
23. Moran, E. C., Chou, P. Y., and Fasman, G. D. (1977) Conformational transitions of glucagon in solution: The α to β transition, *Biochem. Biophys. Res. Commun. 77*, 1300−1306.
24. Pedersen, J. S., Dikov, D., Flink, J. L., Hjuler, H. A., Christiansen, G., and Otzen, D. E. (2006) The changing face of glucagon fibrillation: Structural polymorphism and conformational imprinting, *J. Mol. Biol. 355*, 501−523.
25. Pedersen, J. S., Flink, J. M., Dikov, D., and Otzen, D. E. (2006) Sulfates dramatically stabilize a salt dependent type of glucagon fibrils, *Biophys. J. 90*, 4181−4194.
26. Unson, C. G. (2002) Molecular determinants of glucagon receptor signaling, *Biopolymers 66*, 218−235.
27. Pace, C. N., and Vanderburg, K. E. (1979) Determining globular protein stability: Guanidine hydrochloride denaturation of myoglobin, *Biochemistry 18*, 288−292.
28. Pace, C. N. (1986) Determination and analysis of urea and guanidine hydrochloride denaturation curves, *Methods Enzymol. 131*, 266−280.
29. Forster, V. T. (1948) Zwischenmolekulare Energiewanderung und Fluoreszenz (Intermolecular energy migration and fluorescence), *Ann. Phys. (Weinheim, Ger.) 437*, 55−75.
30. Hatters, D. M., MacPhee, C. E., Lawrence, L. J., Sawyer, W. H., and Howlett, G. J. (2000) Human apolipoprotein C-II forms twisted amyloid ribbons and closed loops, *Biochemistry 39*, 8276−8283.
31. Bromer, W. W., Staub, A., Diller, E. R., Bird, H. L., Sinn, L. G., and Behrens, O. K. (1957) The Amino Acid Sequence of Glucagon, *J. Am. Chem. Soc. 79*, 2794−2798.
32. Ferrone, F. (1999) Analysis of protein aggregation kinetics, *Methods Enzymol. 309*, 256−274.
33. Munishkina, L. A., Henriques, J., Uversky, V. N., and Fink, A. L. (2004) Role of protein-water interactions and electrostatics in α-synuclein fibril formation, *Biochemistry 43*, 3289−3300.
34. Fersht, A. R., and Sato, S. (2004) ϕ-value analysis and the nature of protein-folding transition states, *Proc. Natl. Acad. Sci. U.S.A. 101*, 7976−7981.
35. Otzen, D. E., Kristensen, O., and Oliveberg, M. (2000) Designed protein tetramer zipped together with a hydrophobic Alzheimer homology: A structural clue to amyloid assembly, *Proc. Natl. Acad. Sci. U.S.A. 97*, 9907−9912.
36. Kieffer, T. J., and Habener, J. F. (1999) The glucagon-like peptides, *Endocr. Rev. 20*, 876−913.
37. Onoue, S., Iwasa, S., Kojima, T., Katoh, F., Debari, K., Koh, K., Matsuda, Y., and Yajima, T. (2006) Structural transition of

glucagon in the concentrated solution observed by electrophoretic and spectroscopic techniques, *J. Chromatogr., A 1109*, 167−173.
38. Wu, C. S., and Yang, J. T. (1980) Helical conformation of glucagon in surfactant solutions, *Biochemistry 19*, 2117−2122.
39. Street, A. G., and Mayo, S. L. (1999) Intrinsic β-sheet propensities result from van der Waals interactions between side chains and the local backbone, *Proc. Natl. Acad. Sci. U.S.A. 96*, 9074−9076.
40. Chou, P. Y. f., and Fasman, G. D. (1975) The conformation of glucagon: Predictions and consequences, *Biochemistry 14*, 2536−2541.

BI061228N